PHYSICAL REVIEW B VOLUME 40, NUMBER 13 1 NOVEMBER 1989

Monte Carlo study of the W(001) surface reconstruction transition based on total-energy calculations

L. D. Roelofs, T. Ramseyer, and L. L. Taylor
Physics Department, Haverford College, Haverford, Pennsylvania 19041

D. Singh
Naval Research Laboratory, Washington, D.C. 20375

H. Krakauer
Physics Department, College of William and Mary, Williamsburg, Virginia 23185

(Received 4 May 1989)

We describe the extraction from local-density-approximation-based total-energy calculations of the potential governing the reconstruction of the W(001) surface and an extensive Monte Carlo simulation investigation thereof. Our study is successful in reproducing the qualitative features of this much-studied surface reconstruction, in particular confirming and fully characterizing its order-disorder character. We find and discuss a discrepancy with the measured transition temperature, concluding that it probably arises from remaining small inaccuracies in the total-energy calculations.

I. INTRODUCTION

Interest in the surface reconstruction of W(001) remains considerable even 20 years after its basic nature was first discussed and elucidated.[1-3] Theoretical interest continues because the subtlety of the electronic driving forces represents a challenge of understanding and a test of accuracy of various approaches to electronic-structure calculations.[4-8] Increasingly finely honed experimental studies[9-15] offer more detailed pictures of various aspects of the transition. Yet some basic theoretical questions remain at issue, especially centering on the significance of Fermi surface states to the reconstruction. Early theoretical work focused on charge-density-wave-type mechanisms.[16-18] Subsequent studies suggested a Jahn-Teller–like mechanism involving states throughout the d bands,[19] a picture which was supported by local-density-approximation-based (LDA) total-energy calculations.[4] Most recently pseudopotential studies[8] comparing the W(001) and Mo(001) surfaces—the latter exhibits a similar but incommensurate reconstruction—have revived questions about the significance of longer-range, Fermi-surface mechanisms.

In this situation of competing interpretations of mechanism, it is important to make the contact between theoretical and experimental studies as close as possible. The most accurate electronic-structure calculations are restricted to small unit cells and thus to very orderly ($T=0$) situations. They can thus predict the character of the ordered state but not the transition temperature or the character of the phases in the transition region. Experimental studies, on the other hand, usually focus on the transition regime ($T_c=210$ K).[9] In this paper we discuss a combination of electronic-structure total-energy calculations with Monte Carlo simulations that allows efficient access to the transition region. The method depends on the extraction of the parameters of a classical Hamiltonian governing the motion of the surface-layer atoms from the total-energy calculations. If the assumed form of that Hamiltonian adequately describes the system and if sufficiently diverse total-energy calculations support the extraction of parameters then this approach can accurately model the system near the transition temperature, thus allowing more direct confrontation between theory and experiment and providing a check of the accuracy of the underlying first-principles method.

This approach has the additional attractive feature that, if successful, it identifies the specific interactions most responsible for driving the reconstruction. This could be helpful in characterizing the reconstruction mechanism.

In this work we assume a short-range interaction model and show that its parameters can be extracted from total-energy electronic-structure calculations in just a few orderly (small unit cell) configurations. We then study the resulting model via Monte Carlo simulations.

II. HAMILTONIAN

Our method begins with the assumption of a Hamiltonian specifying the total energy of the surface region as a function of atomic positions. In this first attempt we focus on the energetics of just the first (surface) layer, including explicitly the interactions within that layer and its interactions with underlying layers which are assumed to be static except for random thermal motion. This represents in effect a spatial truncation of the interaction in the direction normal to the surface. The other physically relevant terminations of the Hamiltonian are the range of the interactions parallel to the surface and the highest order of the terms included. In the present effort we have included symmetry-allowed terms up to fourth

order,[20] which allows an accurate account for all energetic features found from the slab calculations.[5]

The specific form we have chosen is

$$H = H_{\text{loc}} + H_{\text{int}} + E_0 \ , \tag{1}$$

where E_0 is an arbitrary energy zero,

$$H_{\text{loc}} = \sum_i \left[\tfrac{1}{2} A u_i^2 + \tfrac{1}{4} B u_i^4 + \tfrac{1}{2} V_4 u_i^4 \cos(4\theta_i) + \tfrac{1}{2} A_z (z_i - z_0)^2 + V_z u_i^2 z_i \right] \tag{2a}$$

(H_{loc} describes the interactions of surface layer atoms with underlying layers) and

$$H_{\text{int}} = \sum_{\langle ij \rangle_1} \{ J_1 \mathbf{u}_i \cdot \mathbf{u}_j + K_1 S_{ij} (u_{ix} u_{jx} - u_{iy} u_{jy}) + R_1 [u_{ix} u_{jx} (u_{ix}^2 + u_{jx}^2) + u_{iy} u_{jy} (u_{iy}^2 + u_{jy}^2)] \} + \sum_{\langle ij \rangle_2} J_2 \mathbf{u}_i \cdot \mathbf{u}_j \tag{2b}$$

(H_{int} specifies the interactions within the surface plane). In Eqs. (1) and (2) $\mathbf{u}_i$ is a 2D vector representing the displacement of the surface atom at site i parallel to the surface plane (u_i is the magnitude of this vector and u_{ix} is its x component), z_i is the displacement of that atom normal to the plane (positive outward), $\langle ij \rangle_k$ denotes an kth neighbor pair of sites in the surface plane, and $S_{ij} = 1$ (-1) if sites i and j are displaced from one another in the x (y) direction. $A, B, V_4, \ldots J_1, \ldots J_2$ are parameters to be specified.

Having chosen this form for H we proceed to determine the parameter values via least-squares fitting of the calculated total energies to the assumed Hamiltonian. These energies were determined as described in Singh and Krakauer,[5] for a variety of in-plane and normal displacement patterns (characterized by the 2D periodicity and displacement direction) and magnitudes. Besides the arrangement characterized by normal shifts only, patterns of character $\Gamma\langle 10 \rangle$, $\Gamma\langle 11 \rangle$, $M\langle 10 \rangle$, $M\langle 11 \rangle$, $X\langle 10 \rangle$, and $X\langle 01 \rangle$ were considered. [In this notation for the displacement patterns the first character gives the point in the surface Brillouin zone that defines the periodicity; the following vector gives the direction of the local displacements—see Fig. 1(a). Note that the Γ and M patterns are invariant with respect to 90° rotations of all displacements while the X patterns are not.] For each pattern calculations were done for a variety of displacement magnitudes at one particular choice for the normal shift of the last plane such that the energy minimum of that particular pattern is traversed. Six other configurations along the $M\langle 11 \rangle$ energy trough [see Fig. 2(a)] were also used. For all calculations the positions of second-layer and deeper atoms were constrained to the bulk locations. About 50 distinct energies were calculated altogether.

We then determined the parameters in Eqs. (1) and (2) using a weighted (to favor the most likely displacement patterns) least-squares fit. The resultant values are given in Table I. The Hamiltonian with fitted parameters accurately reproduces the calculated energies as can be seen in Fig. 1. Once its parameters have been determined, the Hamiltonian specifies the energy as a function of any displacement pattern and magnitude. For example, the dependence of the energy on in-plane displacement magnitude and first-layer relaxation in the $M\langle 11 \rangle$ pattern is shown in the form of a contour plot in Fig. 2. Equations (1) and (2) also contain information concerning the energy of less orderly arrangements and so form the basis for the Monte Carlo simulation we discuss in Sec. III.

Other groups have attempted to model this phase transition. The veracity of treatment depends on the potential used so it is worth commenting on similarities and differences. Studies by Ying and co-workers[21,22] have been based on a model with 2D displacements lacking amplitude fluctuations (atomic displacements are fixed in magnitude) and so are useful for describing the critical behavior of the model, but cannot give a quantitative account of the nature of the phases or the transition temperature. The study of Roelefs and Wendelken[23] was based on models with amplitude fluctuation, but allowed displacements only within the surface plane. This approach allowed discussion of the nature of the phases involved, but since the potentials were not determined from total energy calculations, could not determine T_c. (In that work two disparate models were studied; the potential used in the present work is closer to the one termed Model I.) Tosatti and co-workers have made extensive lattice-dynamical[24] and molecular-dynamics[25] studies of a model including amplitude fluctuations and allowed displacements in the direction perpendicular to the surface. Their potential[24] is derived from bulk information with *ad hoc* modification of surface-layer force constants to account for the observed reconstruction and its transition temperature. The most important differences between their potential and that used in the present work are in the interactions between surface-layer atoms and underlying layers, the contribution H_{loc} in Eq. (1). In the potential of Fasolino and Tosatti these terms are bulklike and so oppose any reconstruction. The observed $c(2\times 2)$ reconstruction must then be driven completely by interactions within the surface layer. In our fitting procedure the parameter A turns out to be negative, indicating that the interaction between first- and second-layer atoms favors all reconstruction modes. (But because of its lack of selectivity, it does not influence the transition temperature of any one mode very significantly.) This difference leads to very significant quantitative differences between the character of the phases in the transition region and to a very different ratio of T_c to reconstruction energy. Another but less significant difference between the two potentials is manifested in the relaxation of the surface layer perpendicular to the surface. Due again to the use of bulklike terms for the first- and second-layer interactions, their relaxation is outward in both reconstructed and unreconstructed surfaces. In contrast, most total energy calculations indicate inward relaxation as included in our potential. The potentials are in rather close agreement as to the degree of anisotropy defined below in Eq. (6).

III. SIMULATION

Our simulation code considers one active layer of atoms assigned to sites in an $(N\times N)$ square array with

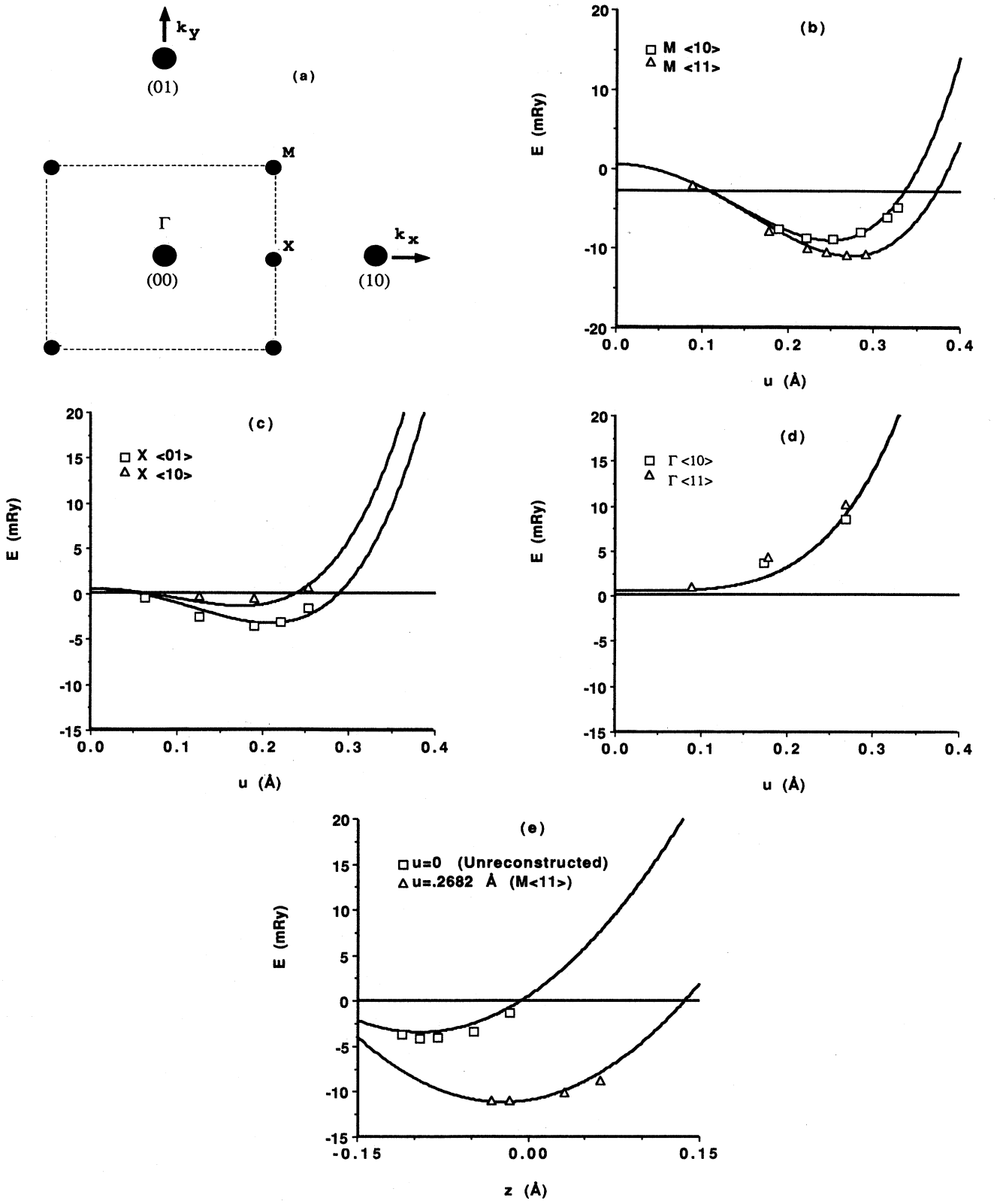

FIG. 1. Definition of displacement patterns for which total-energy calculations were performed and the fit of the Hamiltonian in Eqs. (1) and (2) to them. (a) 2D surface Brillouion zone with high symmetry points indicated. (b)–(e) Hamiltonian fit for displacement patterns as indicated in the panels; plotted points are total energies calculated as in Ref. 3 and curves depict the variation of the total energy with displacement magnitude from Eqs. (1) and (2) based on fitted parameter values.

periodic boundary conditions. The standard Metropolis algorithm is used for accepting or rejecting attempted displacements of individual atoms which are 3D moves, randomly chosen within a volume whose base is 0.4 Å^2 and whose height is 0.09 Å. (These limits allow a given atom to completely reverse its displacement, but still give reasonable acceptance rates.) The propagation loop is vectorized for efficient processing on a CRAY supercomputer. Run lengths varied with proximity to the transition and lattice size. Our larger lattices (48×48) had to be run to a length of 100 000 attempted moves per site near the critical point. Periodically the simulation was interrupted to calculate experimental observables including the (kinematic) diffraction intensity,[26] the energy and the separate contributions thereto from the terms in Eq. (2), average displacement magnitudes and anisotropy, degree and nature of disorder, etc.

In the real experimental system, the atomic displacements characteristic of the reconstruction are confined mostly to the top layer[13]—hence our use of a Hamiltonian dependent on first-layer displacements only. However, even if the second and underlying layers have little role in driving the reconstruction, they still may have an important influence on first-layer movements via thermal disorder. We simulate this effect by adding stochastic perturbations to $H_{\rm loc}$, since that part of the Hamiltonian describes the interaction between a given surface-layer atom and the nearby underlying atoms. For simplicity, we focus on the four second-layer atoms closest to a given top-layer atom and let $\mathbf{d}_t=(\Delta u_x,\Delta u_y,\Delta z)$ denote an effective, time-dependent change of origin in $H_{\rm loc}$, due to the thermal displacements of the four atoms. We assume that the three components of $\mathbf{d}_t$ fluctuate randomly with the amplitude expected from bulk Debye behavior.[27] This variation of second-layer positions couples to first-layer energetics in the form of an addition to $H_{\rm loc}$ which we have termed $H_{\rm pert}$. For example, the term $\frac{1}{2}Au_i^2$, in Eq. (2a) generates a contribution $(-A\mathbf{d}_t\cdot\mathbf{u}_i)$ in $H_{\rm pert}$. Then at each simulation step we calculate not only the usual total energy change $\Delta E=H_f-H_i$ associated with the proposed "move" but also a $\Delta E_{\rm pert}$, based on the randomly generated current value of $\mathbf{d}_t$, which reflects the change that occurs in $H_{\rm pert}$ as a result of that move. The probability of accepting the move, $p=\exp[-(\Delta E+\Delta E_{\rm pert})/k_BT]$, includes the thermal contribution.

With this simulation code we have investigated the phase transition, focusing on the dependence on lattice size, the characteristics of the transition region, and the

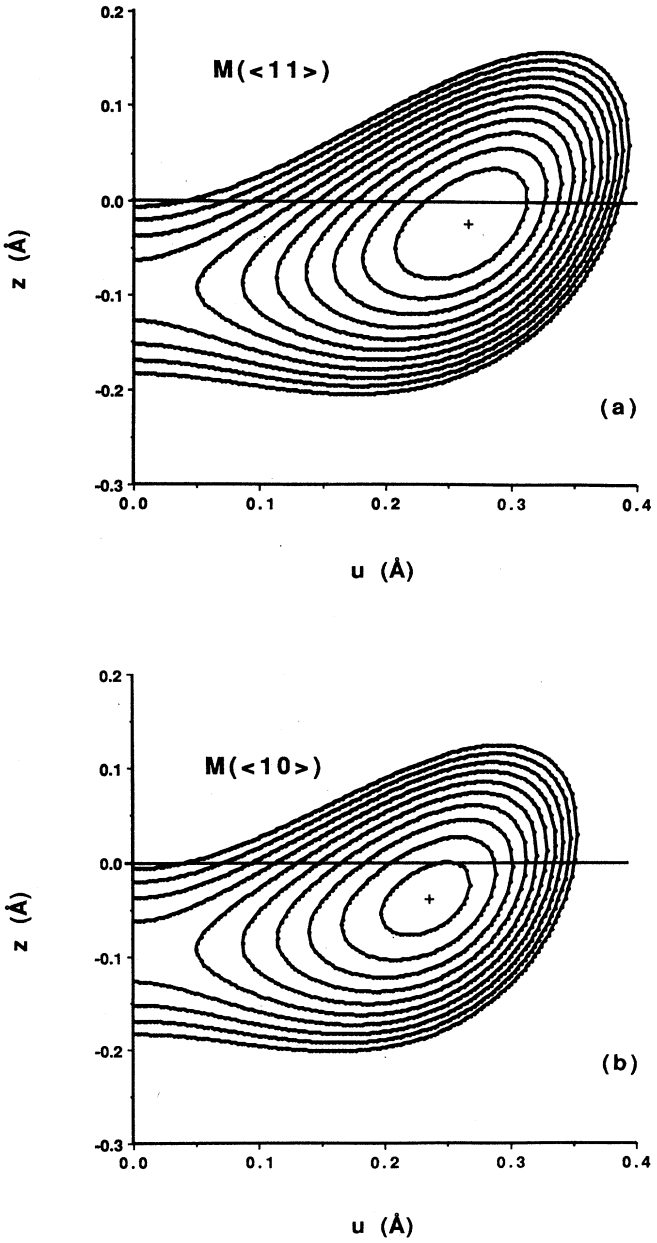

FIG. 2. Contour plots of the total energy vs displacement magnitude, in the plane u and perpendicular to the surface z for displacement patterns of (a) $M\langle 11\rangle$ character and (b) $M\langle 10\rangle$ character.

TABLE I. W(001) surface Hamiltonian parameters deduced from total-energy calculations.

Local terms	NN terms	NNN term
A, −301.94 mRy/Å^2	J_1, 76.14 mRy/Å^2	J_2, −0.615 mRy/Å^2
B, 7686.67 mRy/Å^4	K_1, 12.86 mRy/Å^2	
V_4, 214.29 mRy/Å^4	R_1, −100.85 mRy/Å^4	
A_z, 882.75 mRy/Å^2	($z_0=-0.095$ Å)	
V_z, −896.82 mRy/Å^3		

effects of inaccuracy in the underlying electronic structure calculations. To locate the transition temperature we considered the most convenient experimental measure of the (square) order parameter, the kinematic diffraction intensity at the position of the extra beams,

$$I_{1/2,\pm 1/2}=\left|\sum_i \exp\left[i\left[\frac{\pi}{a},\pm\frac{\pi}{a}\right]\cdot(\mathbf{R}_i+\mathbf{u}_i)\right]\right|^2 . \quad (3)$$

where $\mathbf{R}_i$ is the location of the ith lattice site and a is the lattice constant. [For the purposes of locating the transition, we have ignored the momentum transfer ($\mathbf{k}$) component perpendicular to the surface. As discussed below we also calculate in each simulation run the kinematic diffraction intensity including the third component of $\mathbf{k}$. Thus we can consider the Debye-Waller behavior of the system and other interesting effects.] Since $|\mathbf{u}| \ll a$, the exponential in Eq. (3) can be expanded, leading to a much more efficient form for the sum,

$$I_{1/2,\pm 1/2}=\left|\frac{\pi}{a}\sum_i S_i(u_{ix}\pm u_{iy})\right|^2 , \quad (4)$$

where $S_i=\pm 1$ depending on which $c(2\times 2)$ sublattice site i is on. In the ordered state either $I_{1/2,1/2}$ or $I_{1/2,-1/2}$ will become nonzero, each one corresponding to one of the two possible directions of displacement, NE-SW or NW-SE. In experimental studies the incident beam is sufficiently large so that many regions of both orientations are illuminated incoherently. Thus both extra beams are typically seen simultaneously. In simulations the orientation of order can rotate abruptly during a temperature scan, particularly in the vicinity of the transition, so that it is convenient to use the (normalized) average of the two (squared) components of the order parameter,

$$I_M \equiv \frac{\frac{1}{2}(I_{1/2,1/2}+I_{1/2,-1/2})}{\left[\frac{\pi}{a}\right]^2} \quad (5)$$

for locating the transition.

We calculate I_M for several temperature scans through the vicinity of the transition, average the separate scans together, and then fit a smooth curve through the calculated points. The inflection point of this curve is taken to mark the transition temperature for a given lattice size.

IV. RESULTS

A. Transition temperature

The model defined by Eqs. (1) and (2) and, by extension, the actual system itself exhibits a phase transition in the universality class of the XY model with cubic anisotropy.[28] This model[21,29] and the system itself[9] have been shown to be unusually sensitive to finite-size effects. We thus studied the transition with three lattice sizes, (12×12), (24×24), and (48×48), so that we could extrapolate to infinite system behavior with some confidence. Figure 3 shows a plot of I_M versus T for these three lattice sizes. The transition temperatures determined according to the above procedure were 523.6, 518.6, and 519.7 K, respectively, so that one may surmise $T_c=510\pm 5$ K. We will discuss the significant discrepancy between this value and the experimental value[9] of 210 K below, focusing first on the qualitative nature of the transition.

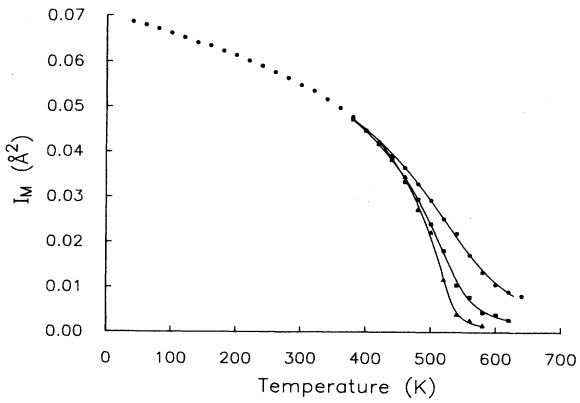

FIG. 3. I_M vs T from Monte Carlo simulation for lattices of size (12×12), circles; (24×24), squares; and (48×48), triangles. Solid curves are fits of the calculated values to a smooth curve with a single inflection point whose position is taken to be T_c in each case. I_M can be taken to be the average of the squares of the two-order parameter components for this model.

B. Nature of transition and phases

Though the nature of the transition and the character of the phase immediately above T_c were once controversial, with some workers arguing for an order-order picture,[30] and others for an order-disorder view,[31] the situation now seems to be settled in favor of the latter.[10,14,15,23] Our short-range interaction Hamiltonian is also consistent only with a disordered phase above T_c. However, with simulations one can do more than label a phase as disordered or ordered. One can also conveniently character the nature and degree of any disorder present. We present in Fig. 4 the variation with temperature of several relevant local quantities through the transition, giving both the ensemble or time average denoted $\langle x\rangle$ for measurable x, and the ensemble average of the *spatial* variance denoted $\langle \sigma_x \rangle$,

$$\sigma_x \equiv \left\{\frac{1}{N^2}\left[\sum_i x_i^2-\left[\sum_i x_i\right]^2\right]\right\}^{1/2} , \quad (6)$$

where x_i is the value of observable x at site i at the simulation step during which accumulation for time average is occurring.

$\langle u^2\rangle$ characterizes the displacement magnitudes irrespective of the degree of order and can be measured by integrating the diffracted kinematic intensity.[14] $\langle z\rangle$ characterizes the average relaxation of the surface plane which can be measured via I-V LEED techniques which take disorder into account.[15] $\langle \sigma_{u^2}\rangle$ and $\langle \sigma_z\rangle$ contribute to measurable Debye-Waller factors. $\langle \cos(4\theta)\rangle$ characterizes the orientation of the order and $\langle \sigma_{\cos(4\theta)}\rangle$ the de-

gree of anisotropy or orientations on the surface, the latter having important ramifications in classifying the transition.

Figure 4(a) shows the variation of $\langle u^2 \rangle$ and $\langle \sigma_{u^2} \rangle$. Note that very substantial displacement magnitudes persist above T_c (marked with the arrow on the temperature scale), and that there is very little variation in the immediate vicinity of the transition. This is consistent with the x-ray-diffraction results of Robinson *et al.*[14] In Fig. 4(b), $\langle z \rangle$ and $\langle \sigma_z \rangle$ are plotted versus temperature. Note that the relaxation of the last layer spacing stays close to what it is in the ordered state. This is not in quantitative agreement with the *I-V* LEED analysis of Pendry *et al.*,[15] which finds a large inward shift of 0.13 Å well above T_c. The reason for the disagreement may lie in the character of disorder assumed in that paper, which in a given calculation is δ-function-like, i.e., $\langle \sigma_{u^2} \rangle = \langle \sigma_z \rangle = \langle \sigma_{|\cos 4\theta|} \rangle = 0$ with disorder only in direction. Figure 4(c) shows the variation with temperature of $\langle \cos 4\theta \rangle$ and $\langle \sigma_{\cos 4\theta} \rangle$. The interesting feature apparent in this plot is that the anisotropy has relatively little effect near the transition. $\langle \cos 4\theta \rangle$ is still very close to 0 and its variance over the lattice at any given time is such that the displacements appear to be rotating freely. One is, in other words, very close to zero anisotropy, giving reason to hope that Kosterlitz-Thouless behavior might be accessible in this system.

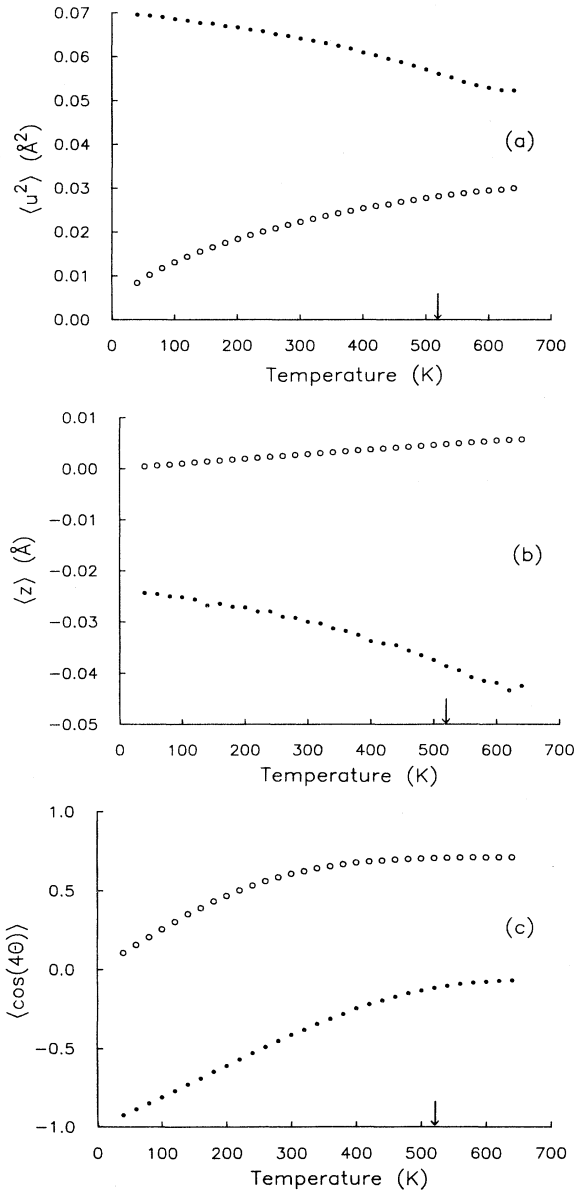

FIG. 4. Variation of local observables through the transition from Monte Carlo simulation. In each case the expectation value (or Monte Carlo "time average") is plotted as the solid point and the time average of the spatial variance (see text) of the same quantity as the open circle.

C. Discussion

We consider next the quantitative accuracy of our treatment of the system in light of the discrepancy between transition temperatures. Although this experimental system is known to be rather sensitive to surface defects, such as steps,[9] and low-coverage contamination,[32–34] we feel that the most likely explanation for the discrepancy lies in shortcomings of our theoretical treatment. The possible explanations include inadequacies of the assumed Hamiltonian form—for example, longer-range interactions may be important, or inaccuracies in the total-energy calculations upon which we based out parameter fits. We have investigated the latter possibility more carefully. We estimate that our general potential LAPW method determines energy differences for different configurations with an accuracy of about 20%. We accordingly investigated the effect of a 20% error on the energy of the Γ displacements, lowering their energy by that amount, leaving the other energies unaltered. The result is an exchange of driving strength between the J_1 and A terms in the Hamiltonian, *but no difference in the reconstruction energy.* (In effect one is transferring driving force from intra-layer effects to interlayer effects.) As can be seen in Fig. 5 this makes a substantial difference in the transition temperature, lowering T_c to about 345 K. There are qualitative effects as well, with the displacement magnitudes $\langle u^2 \rangle$ showing less variation as one passes through T_c. We are led to conclude that most of the discrepancy between experiment and our calculations can be readily accounted for by the small inaccuracies still remaining in state-of-the-art total-energy calculations. The high sensitivity of the transition temperature and other system properties seem to constitute a very precise test of accuracy.

It is worth noting that T_c is not very sensitive to the degree of four-fold anisotropy. A convenient parameter for characterizing the degree of anisotropy is the difference in reconstruction energy in the $M\langle 11 \rangle$ and $M\langle 10 \rangle$ patterns divided by twice the former (this definition is consistent with that typically used for models lacking amplitude fluctuations[35]),

$$H_4 = \frac{E_{\min}(\langle 11 \rangle) - E_{\min}(\langle 10 \rangle)}{2E_{\min}(\langle 11 \rangle)} . \tag{7}$$

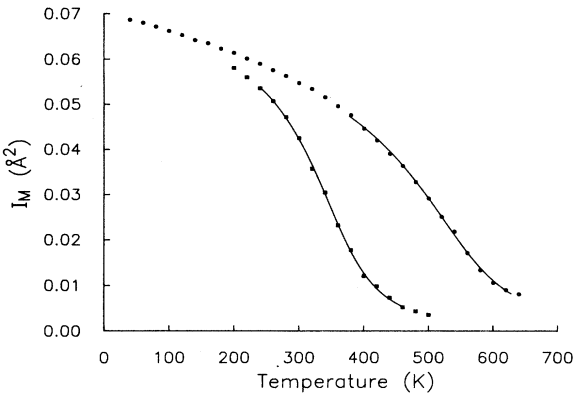

FIG. 5. Plot of I_M vs T from Monte Carlo simulations comparing results from the unperturbed potential and that in which some of the reconstruction energy is transferred from the J_1 term to the A term.

Our potential has $H_4=0.11$. To check the dependence of T_c on H_4 we performed some calculations with anisotropy very close to 0 (by arranging for the effects of V_4 and R_1 to cancel in our potential). T_c was diminished by less than 5% by this change. This is consistent with the expected form of the phase diagram of the XY model with four-fold anisotropy.[31,35]

Fu and Freeman[6] have also carried out total-energy calculations in the FLAPW method for this system. They have reported the energy variation only for the $M\langle 11\rangle$ and $M\langle 10\rangle$ structures so that a full comparison of results is not possible. It should be noted, however, that their reconstruction energy is smaller than ours by a factor of 3 when second-layer atoms are held fixed[7] (as ours were), and doubles when second-layer relaxation is included.[6] The reduction of reconstruction energy would imply, in the zeroth approximation, a reduced value for T_c thus perhaps improving correspondence with experiment. Lacking calculations for other displacement patterns we cannot improve on this crude estimate. The reason for the discrepancies between the two calculations is not presently understood.

Wang *et al.*[25] have also recently investigated the phase transition of clean W(001) via a molecular-dynamics calculation. (Their potential is discussed in Sec. II.) Their calculation includes several layers of W atoms, but is restricted to significantly shorter simulation runs. The qualitative features they find are mostly similar to our results. However, the intrinsic differences between their potential and ours, especially the partition of the driving force between first- and second-layer contributions, give rise to quantitative differences in the behavior of the experimentally accessible quantifies plotted in Fig. 4. Their value for T_c is much closer to the experimental result than ours. This is not surprising given that their potential parameters were adjusted to give agreement with the experimental value.

V. SUMMARY

We have shown that it is possible to make quantitative comparisons between theoretical methods for calculating transition-metal surface energies and interesting experimental surface reconstruction transitions. The degree of correspondence that has been achieved indicates that LDA-based total energy methods are reasonably accurate—at the mRy level—for the treatment of surfaces and provides a detailed verification of experimental characterizations of the nature of the transition and the character of the phases involved.

We have also succeeded in characterizing the degree of anisotropy of orientation to be expected in the vicinity of the transition. This is significant in that it determines how close this system lies to the interesting zero-anisotropy case at which one expects a Kosterlitz-Thouless critical point.[31] (Adsorption of hydrogen allows control of anisotropy,[36] suggesting that it may be possible to realize a KT transition experimentally.)

ACKNOWLEDGMENTS

Useful discussions with Ian Robinson, Peder Estrup, and C.-Z. Wang are gratefully acknowledged. L.D.R. and T.R. were supported under National Science Foundation (NSF) Grant No. DMR-8705568 and H.K. under NSF Grant No. DMR-8719535. This work was partially supported by the National Center for Supercomputing Applications (NCSA) under Grant No. TRA890069N and was performed on the CRAY X-MP/48 system at the University of Illinois at Urbana-Champaign. Additional computations were carried out at the Cornell National Supercomputer Facility.

[1]T. E. Felter, R. A. Barker, and P. J. Estrup, Phys. Rev. Lett. **38**, 1138 (1977).
[2]M. K. Debe and D. A. King, J. Phys. C **10**, L303 (1977).
[3]R. A. Barker, P. J. Estrup, F. Jona, and P. M. Marcus, Solid State Commun. **25**, 375 (1978).
[4]D. Singh, S.-H. Wei, and H. Krakauer, Phys. Rev. Lett. **57**, 3292 (1986).
[5]D. Singh and H. Krakauer, Phys. Rev. B **37**, 3999 (1988).
[6]C. L. Fu and A. J. Freeman, Phys. Rev. B **37**, 2685 (1988).
[7]C. L. Fu, A. J. Freeman, E. Wimmer, and M. Weinert, Phys. Rev. Lett. **54**, 2261 (1985).
[8]X. W. Wang and W. Weber, Phys. Rev. Lett. **58**, 1452 (1987).
[9]J. F. Wendelken and G.-C. Wang, Phys. Rev. B **32**, 7542 (1985).
[10]I. Stensgaard, K. G. Purcell, and D. A. King, Phys. Rev. B **39**, 897 (1989).
[11]E. K. Schweizer and C. T. Rettner, J. Vac. Sci. Techol. (to be published).
[12]B. Salanon and J. Lapujoulade, Surf. Sci. **173**, L613 (1986).
[13]M. S. Altman, P. J. Estrup, and I. K. Robinson, Phys. Rev. B **38**, 5211 (1988).
[14]I. K. Robinson, A. A. MacDowell, M. S. Altman, P. J. Estrup, K. Evans-Lutterodt, J. D. Brock, and R. J. Birgeneau, Phys.

Rev. Lett. **62**, 1294 (1989).
[15]J. B. Pendry, K. Heinz, W. Oed, H. Landskron, K. Müller, and G. Schmidtlein, Surf. Sci. **193**, L1 (1988).
[16]E. Tosatti, Solid State Commun. **25**, 637 (1978).
[17]J. E. Inglesfield, J. Phys. C **12**, 149 (1979).
[18]M. Posternak, H. Krakauer, A. J. Freeman, and D. D. Koelling, Phys. Rev. B **21**, 5601 (1980).
[19]I. Terakura, K. Terakura, and N. Hamada, Surf. Sci. **111**, 479 (1981).
[20]Not all possible fourth-order terms need be included to account for the calculated energetics. To avoid underdetermination of the parameter set we have chosen not to include terms beyond those needed to accurately reproduce the calculated energetics.
[21]G. Y. Hu and S. C. Ying, Physica A **140**, 585 (1987).
[22]K. Kankaala, T. Ala-Nissila, and S. C. Ying, Bull. Am. Phys. Soc. **34**, 598 (1989).
[23]L. D. Roelofs and J. F. Wendelken, Phys. Rev. B **34**, 3319 (1986).
[24]A. Fasolino and E. Tosatti, Phys. Rev. B **35**, 4264 (1987).
[25]C. Z. Wang, M. Parrinello, E. Tosatti, and A. Fasolino, Europhys. Lett. **6**, 43 (1988).
[26]We calculated kinematic intensities in two modes. The first assumes little momentum transfer in the direction perpendicular to the surface, modeling a grazing incidence x-ray-diffraction situation. The second mimics the LEED situation, including a substantial Δk in the perpendicular direction.
[27]We assume that the amplitude of thermal displacements varies with $\sqrt{T}$. (The more accurate Debye theory could be used, but our approximation for the effects of thermal disorder is rather crude anyway.) This variation can be calibrated using the measured room-temperature Debye x-ray-diffraction factors. See *International Tables for X-ray Crystallography,* 2nd ed., edited by C. H. Macgillavry and G. D. Rieck (Kynoch, Birmingham, 1968), Vol. III. The room temperature value of the displacement amplitudes in the case of W is about 0.05 Å.
[28]P. Bak, Solid State Commun. **32**, 581 (1979). Our model contains the additional degrees of freedom of amplitude fluctuations and displacements normal to the surface plane. These are thought to be irrelevant.
[29]L. D. Roelofs, Phys. Rev. B **34**, 3336 (1986).
[30]See, for example, D. A. King, Phys. Scr. T **4**, 34 (1983), and references therein.
[31]See, for example, S. C. Ying, and L. D. Roelofs, Surf. Sci. **125**, 218 (1983).
[32]K. Griffiths and D. A. King, J. Phys. C **12**, L755 (1979).
[33]R. A. Barker and P. J. Estrup, J. Chem. Phys. **74**, 1442 (1981).
[34]L. D. Roelofs, J. W. Chung, S. C. Ying, and P. J. Estrup, Phys. Rev. B **33**, 6537 (1986).
[35]J. V. Jose, L. P. Kadanoff, S. Kirkpatrick, and D. R. Nelson, Phys. Rev. B **16**, 1217 (1977).
[36]L. D. Roelofs and S. C. Ying, Surf. Sci. **147**, 203 (1984).